Article

pubs.acs.org/Biomac

Thiol-Mediated Anchoring of Silver Cations to DNA for Construction of Nanofibers on DNA Scaffold

Anatoly A. Zinchenko,*[,†] Ning Chen,[†] Damien Baigl,[‡,⊥,#] Larisa I. Lopatina,[§] and Vladimir G. Sergeyev*[,∥]

[†]Graduate School of Environmental Studies, Nagoya University, Chikusa, Nagoya 464-8601, Japan

[‡]Department of Chemistry, Ecole Normale Supérieure, 24 rue Lhomond, 75005 Paris, France

[§]Department of Colloid Science and [∥]Department of Polymer Science, Faculty of Chemistry, Moscow State University, Moscow, 119899, Russia

[⊥]Université Pierre et Marie Curie, Paris 6, 4 place Jussieu, 75005 Paris, France

[#]UMR 8640, Centre National de la Recherche Scientifique, Paris, France

ABSTRACT: The formation of metal-containing Ag-mercaptoethanol $(-Ag\text{-}S(R)-)_n$ complexes on DNA chain scaffold was studied by UV spectroscopy, zeta potential measurement, and fluorescence and transmission electron microscopies. Experimental results made clear the mechanism of DNA mineralization and compaction, according to which intercalation of silver cations into DNA scaffold and further formation of $(-Ag\text{-}S(R)-)_n$ oligomeric complexes on DNA induce efficient DNA chain compaction by terminal Ag^+ cations. By transmission electron microscopy the formation of fiber-like DNA-templated nanostructures was observed. DNA-Ag-thiol complexes are promising for DNA-templated engineering of hybrid 1D nanostructures with adjustable chemical functionalities by choosing appropriate thiol ligand.

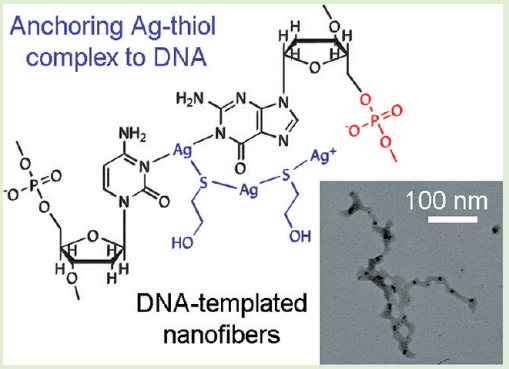

INTRODUCTION

Recently, considerable attention was attracted to the preparation of DNA-based 2D or 3D nanostructures with controlled size, morphology, and composition due to their fundamental interest and potential technological applications.[1−3] During the past decade the utilization of DNA polymer as a scaffold for construction of nanowires was demonstrated in systems of various metals including silver and gold.[4−13] Such nanostructures certainly constitute a promising class of important components for the construction of future electrical, thermoelectrical, optical, chemical, and biochemical devices at nanoscale.[3]

Previous reports showed that interaction of DNA with heavy and noble metals ions, such as Ag^+, Hg^{2+}, and so on, results in intercalation of these metal cations into DNA double helix.[14−17] Ag^+ ion prefers coordinating with DNA bases to electrostatic binding with DNA phosphates,[17] and such coordination with DNA bases has three modes of binding.[16] At low Ag/nucleotide ratios, type I complex is formed with the guanine N7 atom as a major binding site and adenine N7 site at higher concentrations. At ratios of Ag/nucleotide 0.2 to 0.5, type II complexes are formed with A-T or G-C base pairs as main binding targets. Finally, at ratios above 0.5, type III complexes are formed when the major binding sites in type I and type II complexes are saturated.[16] Thiols are well known as effective complexing agents for Ag^+,[18,19] and silver ion and thiol form 1d nanostructures consisting of polymerized $(-Ag\text{-}S(R)-)_n$ sequences of either positive or negative charge.[20−26] Therefore, it is suggested that interaction of Ag^+ with DNA can be utilized to initiate the formation of complexes between Ag^+ and thiols growing along DNA chain. In this work, we investigated DNA-templated growth of $(-Ag\text{-}S(R)-)_n$ structures and studied DNA conformation behavior and the morphology of resulted nanostructures.

EXPERIMENTAL PART

Materials. Bacteriophage T4 DNA (166.000 base pairs, Nippon Gene, Japan), salmon sperm DNA (Wako Chemicals, Japan), $AgNO_3$ (99.9999% purity, Sigma-Aldrich, Japan), and fluorescent dye YOYO-1 (1,1′-(4,4,7,7-tetramethyl-4,7-diazaundecamethylene)-bis-4-[3-methyl-2,3-dihydro-(benzo-1,3-oxazole)-2-methylidene]-quinolinium tetraiodide) (Molecular Probes, USA) were used. Sodium borohydride, 2-mercaptoethanol, ethanol, sodium sulfide, and other chemicals were purchased from Nacalai Tesque, Japan and used for this study as received.

Sample Solutions. Special precautions were taken to prevent the silver ion complexation, reduction, or precipitation by the chemicals used for sample preparation. For this purpose, DNA solutions for UV spectroscopy and fluorescence microscopy experiments were prepared in Milli-Q water without the addition of salt or buffer. Because concentrated T4 DNA stock (1 mM) is commercially available as a buffered solution (10 mM Tris-HCl (pH 7.5) and 1 mM EDTA), after dilution, T4 DNA sample solutions always contained small amounts of EDTA and Tris.

Received: February 21, 2012
Revised: April 17, 2012

dx.doi.org/10.1021/bm300277f | *Biomacromolecules* XXXX, XXX, XXX−XXX

Fluorescence Microscopy. Fluorescence microscopy observations were performed on a fluorescence microscope (Nikon, TE2000-E) equipped with a 100× magnification oil-immersed lens and recorded on DVD through a Hamamatsu SIT TV camera. Fluorescence images were recorded using an EB-CCD camera and an image processor Argus 10 (Hamamatsu Photonics, Hamamatsu, Japan).

UV−vis Spectroscopy. UV−vis spectra were recorded on a Jasco U-550 UV/vis spectrophotometer in 1.0 × 0.2 × 0.5 cm quartz cells at room temperature.

Transmission Electron Microscopy. Sample solutions for transmission electron microscopy (TEM) were prepared in the same manner as for FM observations. TEM observations were performed at room temperature using a JEM-1200 EX microscope (JEOL, Tokyo, Japan) at an acceleration voltage of 100 kV. We used carbon-coated grids with a mesh size 300. Each grid was placed for 3 min on top of a 15 μL droplet of sample solution on a Parafilm sheet and blotted using paper filter prior to microscopy observation. Observations were made without staining agent.

Elemental Analysis. Elemental analysis of DNA complexes was performed on scanning electron microscope JSM-5600 (JEOL) equipped by energy-dispersive spectrometry system "Voyager", Noran Instruments, USA.

Zeta-Potential Measurements. Zeta potential of silver-mercaptoethanol complexes was measured on Zetatrac (Microtrac, USA).

RESULTS AND DISCUSSION

Complexes of DNA with Silver Ion and Mercaptoethanol. Interaction of salmon sperm DNA with silver nitrate and mercaptoethanol (ME) was studied by UV−vis spectroscopy. Spectra of initial 1×10^{-4} M DNA (in phosphates) in nonbuffered Milli-Q water solution before and after the addition of 1×10^{-3} M of silver nitrate are shown in Figure 1, where the black spectrum (1) corresponds to the absorbance

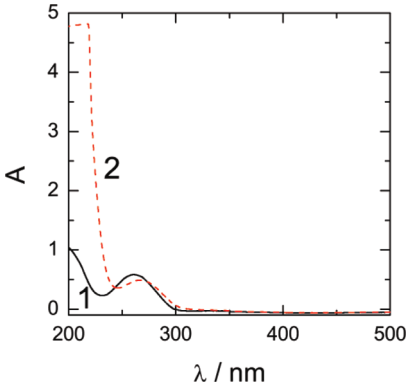

Figure 1. UV−vis absorption spectra of 1×10^{-4} M salmon sperm DNA solution before (1, solid line) and after the addition of 1×10^{-3} M of $AgNO_3$ (2, dashed line).

of free DNA (λ_{max} = 260 nm) and the red curve (2) corresponds to the absorbance of sample after the addition of 10-fold excess of $AgNO_3$ against DNA phosphates. The red shift of the DNA absorbance peak to 280 nm results from silver intercalation into the DNA double helix.[14] Centrifugation of the resulted solution at 10 000 rpm for 10 min has no effect on the intensity of DNA UV absorbance, indicating that all DNA remains in solution. Figure 2 shows the spectra of DNA mixed with 10-fold excess of $AgNO_3$, as described above in the presence of various amounts of ME before and after centrifugation. At low concentrations of ME (1×10^{-5} M, Figure 2A), no change in the original DNA-Ag spectrum was observed after the addition of ME, and after centrifugation the

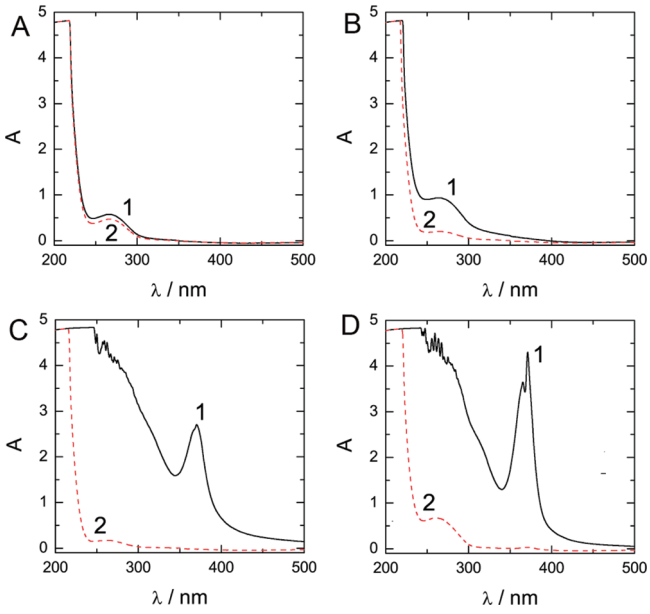

Figure 2. UV−vis spectra of 1×10^{-4} M salmon sperm DNA and 1×10^{-3} M of $AgNO_3$ solution at different concentrations of added mercaptoethanol (A, 1×10^{-5} M; B, 1×10^{-4} M; C, 1×10^{-3} M; D, 1×10^{-2} M) before (1, solid line) and after (2, dashed line) centrifugation.

spectrum of the remained supernatant was similar to the original spectrum. Increase in ME amount (1×10^{-4} M, Figure 2B) caused the increase in absorption intensity in 250−300 nm region, which is attributed to the formation of coordinated $(-Ag\text{-}S(R)-)_n$ complexes.[18−26] After centrifugation of the sample, a decrease in the supernatant optical density at 260 nm was observed, indicating that most of DNA and silver complex was removed from the solution. The addition of the equimolar to Ag^+ amount of ME (1×10^{-3} M, Figure 2C) gives rise to a new intensive peak at 380 nm and strong increase in absorbance in the whole measured spectrum range, which was previously interpreted to occur because of the formation of both bicoordinated and tricoordinated Ag complexes with ME.[27] After centrifugation of this solution (Figure 2C), no significant absorbance at 260 nm was observed again because of the complete removal of DNA and silver-thiol complex from sample solution. Further addition of ME concentration (1×10^{-2} M, Figure 2D) results in the growth of adsorption at 380 nm; however, in contrast with solutions B and C, after centrifugation, DNA remained in solution at its initial concentration (Figure 2D, dashed line), whereas silver complex precipitated. A more detailed precipitation analysis indicates that precipitation of DNA is the most efficient at about the double concentration of ME as compared with $AgNO_3$.

Because in DNA interaction the charge on DNA binder plays an important role; next, we measured the charge on $(-Ag\text{-}S(R)-)_n$ complexes at different ratios of $AgNO_3$ (1×10^{-4} M) to ME. Zeta potential measurements indicate that the charge on $(-Ag\text{-}S(R)-)_n$ complex depends on the ratio between the components, as shown in Figure 3. The complex is positively charged at equivalent ratio of $AgNO_3$ to ME but turned to be almost neutral at 2 and higher ratios of ME and even slightly negatively charged at 10 times excess of ME. These data support the results of UV spectroscopy, according to which positively charged species at 1:1 ratio of silver and thiol cause DNA precipitation (Figure 2C) due to electrostatic neutraliza-

dx.doi.org/10.1021/bm300277f | Biomacromolecules XXXX, XXX, XXX−XXX

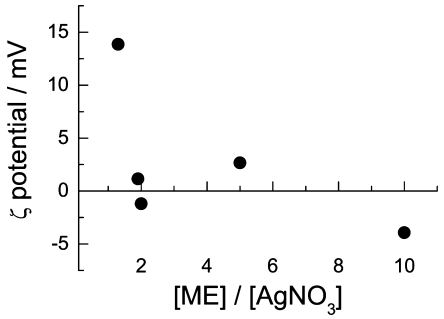

Figure 3. Zeta potential of complexes between ME and $AgNO_3$ at various ratios of ME to $AgNO_3$ concentrations. Concentration of $AgNO_3$ was 1×10^{-4} M.

tion, but no precipitation of DNA occurs in the excess of ME (Figure 2D) corresponding to the formation of the complex of negative charge.

For quantitative evaluation of the composition of the complexes among DNA, $AgNO_3$, and ME after precipitation under conditions as in Figure 2C, the three-component complex was separated by decantation and dried, and Ag, S, and P contents in complexes was analyzed by EDS-equipped scanning electron microscope. It was found that the insoluble complex contained 24 mol % of S, 15 mol % of P, and 62 mol % of Ag, respectively. The most important finding was that complexes are enriched by Ag component by about two-fold in comparison to thiol.

Highly Efficient Single-Molecule DNA Compaction by $AgNO_3$ in the Presence of Thiols. To visualize the interaction of DNA with $AgNO_3$ and ME, we performed single-molecule observations of T4 DNA (166 000 base pairs, contour length ca. 56 μm) by fluorescence microscopy (FM). Similarly to UV spectroscopy measurements, we performed FM observations in nonbuffered aqueous solutions of T4 DNA to prevent Ag^+ ion from complexation with buffer components, but it is important to note that under conditions of single-molecule DNA observations (DNA concentration 1×10^{-8} M) partial denaturation of DNA might take place. First, we studied the effect of $AgNO_3$ on DNA in solution without ME. Figure 4A shows changes in the fluorescence profile of a single DNA molecule labeled by YOYO fluorescent dye after the addition of $AgNO_3$. Up to the 1000-fold excess of $AgNO_3$ to DNA phosphates we did not observe any significant change in DNA conformation, whereas further increase in $AgNO_3$ concentration was accompanied by a slight shrinking of DNA molecules. At higher concentrations of $AgNO_3$ (1×10^{-3} M) the fluorescence image of DNA could not be visualized, which might be due to the replacement of YOYO fluorescent dye from DNA helix as a result of intercalation of silver ions into DNA helix.[14,16] It should be noted that the DNA binding site and DNA conformational changes induced by Ag^+ are drastically different from those induced by alkali ions such as Na^+ or K^+, as we previously discussed.[28]

To get statistically relevant results, we measured a long-axis length (the longest length in the outline of DNA fluorescence image) of at least 100 individual molecules for each $AgNO_3$ concentration. Figure 5 (curve 1) shows the mean long-axis length and statistical error as a function of $AgNO_3$ concentration. At 10 000-fold excess of $AgNO_3$ to DNA phosphates, the long-axis length of the DNA coil decreases by about half of the original length, which is in agreement with our previous study.[28] When the same experiment was performed in the presence of ME, we found dramatic conformational changes in DNA molecules (Figure 4B). Even at equimolar amounts of DNA phosphates and silver ions (1×10^{-8} M) in the presence of ME, significant shrinking of DNA coil was observed. Further increase in $AgNO_3$ and ME

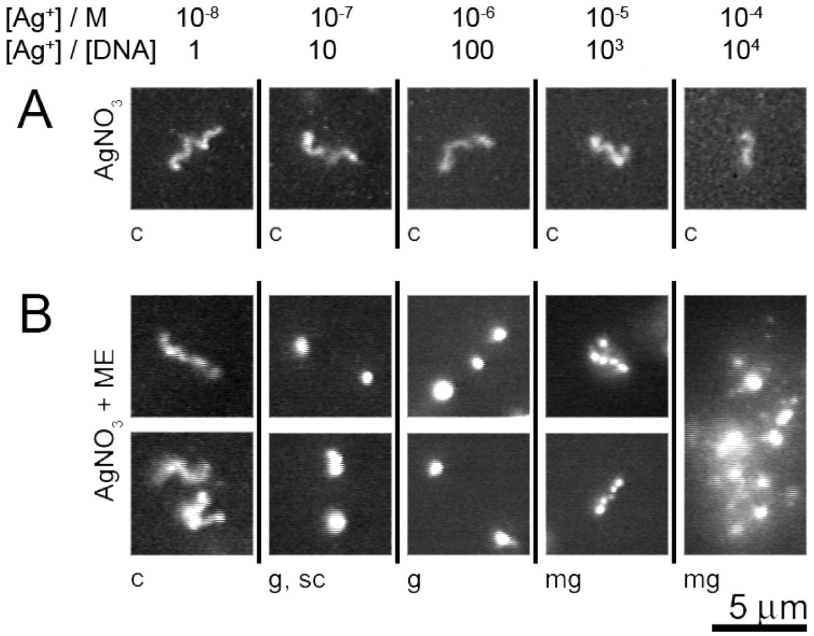

Figure 4. Fluorescence images of single T4 DNA molecules (1×10^{-8} M) at different concentrations of $AgNO_3$ (A) and $AgNO_3$ with ME (B). The letters below the fluorescence images indicate the most frequently observed conformations of individual DNA molecules: c, coil; sc, shrunken coil; g, globule; and mg, multiglobule aggregate. When two abbreviations appear, the former corresponds to a more probable state. The set of two images in panel B is chosen for the purpose of a more complete illustration only. Solutions were prepared by mixing $AgNO_3$ solution with DNA solution of concentration 1×10^{-8} M and further addition of equivalent to $AgNO_3$ amount of ME.

dx.doi.org/10.1021/bm300277f | Biomacromolecules XXXX, XXX, XXX–XXX

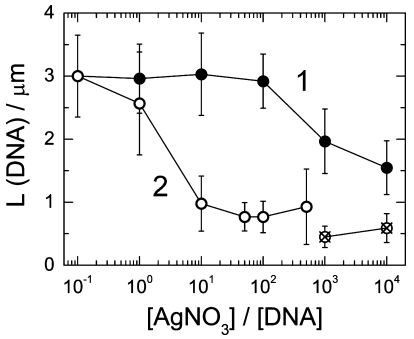

Figure 5. Dependence of the long-axis length (L) of individual T4-DNA molecules (averaged on ca. 100 molecules) on the $AgNO_3$ concentration (closed circles) and $AgNO_3$ concentration in the presence of the equivalent concentration of ME (void circles). Crossed circles indicate the formation of multiglobule aggregates and correspond to the size of globule's images in such aggregates. Sample solutions were prepared by the addition of $AgNO_3$ into the DNA solution (1×10^{-8} M) and further addition of ME. Symbols on plot indicate the maxima of DNA length distributions; the statistical error of the distribution is given as a standard deviation.

concentration leads to a progressive DNA compaction into globular species and then the formation of multiglobular aggregates (multiply globular species assembled into network-like aggregates). The overall size of the aggregates tends to increase with an increase in silver ion concentration and reaches several micrometer size at concentrations 1×10^{-4} M. Control experiments with pure ME and mixture of ME and NaCl (instead of $AgNO_3$) were performed, and it was found that no DNA compaction occurs even at 1×10^{-4} M concentrations of ME or the mixture of NaCl and ME. It should also be noted that the formation of $(-Ag\text{-}S(R)-)_n$ complexes is accompanied by a proton release;[29] therefore, at high concentrations of $AgNO_3$ and ME (1×10^{-4} M), the change of pH might have an influence on the DNA conformational behavior, which, however, excluded at the 10^{-7} M concentrations of $AgNO_3$ and ME, at which DNA compaction was observed.

Figure 5 (curve 2) shows the dependence of DNA long-axis length on the concentration of $AgNO_3$ in the presence of ME. It indicates that the combined action of $AgNO_3$ and ME induces effective compaction of DNA molecules starting from $AgNO_3$ to DNA phosphate ratios as low as 10.

To elucidate the influence of ratio between $AgNO_3$ and ME on the efficiency of DNA compaction, we added various concentrations of ME to the solution of DNA and $AgNO_3$ (1×10^{-8} and 1×10^{-6} M, respectively), and FM observations were performed. When concentration of ME was lower than the concentration of $AgNO_3$ (1×10^{-7} and 1×10^{-8} M), we found that all DNA molecules were in a coil state. At equivalent, 10- and 100-fold excess of ME to $AgNO_3$, globules, and soluble (stable colloid particles in solution) multiglobular aggregates at higher concentrations were found. These results show that for the efficient compaction of the DNA at least an equivalent or higher ratios of the ME to $AgNO_3$ is required; however, the large excess of silver and ME favors the aggregation mechanism of DNA compaction in contrast with single-molecule DNA compaction at concentrations comparable to concentration of DNA.

Mechanism of DNA Compaction in the Presence of $AgNO_3$ and ME. According to the literature and the results obtained in the present study, we propose the following mechanism of $(-Ag\text{-}S(R)-)_n$ complexes formation on DNA scaffold and compaction. According to literature,[16,17] at ratios of Ag to DNA phosphates 1:1, as in our study, silver ion interacts with DNA by intercalation mechanism, penetrating into DNA double-helix and forming complexes with nitrous bases of AT of GC base pairs, as shown in Figure 6A. Because

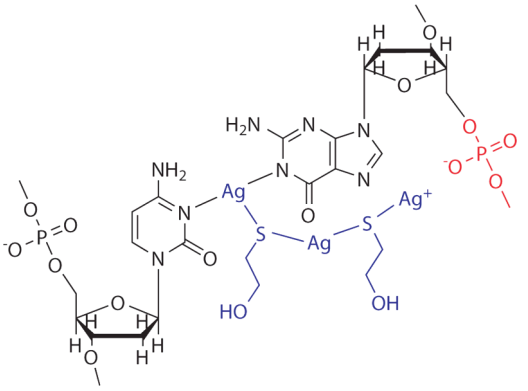

Figure 6. Schematic illustration of the proposed complex structure among DNA, silver, and thiol, in which silver atoms are coordinated with thiol groups and nitrogens of DNA nitrous bases.

Ag^+ can form oligomeric structures with ME,[19,30] intercalation of Ag^+ into DNA accompanied by the formation of $(-Ag\text{-}S(R)-)_n$ complex results in the growth of $(-Ag\text{-}S(R)-)_n$ complex outward DNA helix along the DNA polymeric chain. Importantly, in the process of $(-Ag\text{-}S(R)-)_n$ oligomer growth, terminal Ag^+ ends form ionic bonds with DNA negatively charged phosphates (Figure 6), which causes DNA charge neutralization and compaction, as was observed in FM experiments.

Further evidence of the above proposed mechanism was obtained in the following experiments. ME is a strong ligand for silver ion (pK_{sp} ca. 19.6);[31] therefore, sulfur atom in ME plays a crucial role in the formation of complexes at very low concentrations of silver. By fluorescence microscopy observations, it was confirmed that replacement of ME by the same amount of ethanol induced no DNA compaction, whereas the addition of $NH_2CH_2CH_2SH$, having −SH group, behaved similarly to ME. Therefore, according to these data and the proposed structural model of the complexes between silver ion and ME, the presence of thiol is required for the construction of DNA−silver−ME complexes. Therefore, a broad variety of thiols can be used to build $(-Ag\text{-}S(R)-)_n$ three-component complexes on DNA.

To demonstrate the importance of primary DNA-Ag^+ complex formation for the construction of $(-Ag\text{-}S(R)-)_n$ complex on DNA and its compaction, we performed an reverse experiment, in which we first mixed $AgNO_3$ and ME to form complex $(-Ag\text{-}S(R)-)_n$ and then added this complex to DNA. The comparison of the DNA conformational state change in these two mixing order cases is presented in Figure 7. It is clear that the change in the mixing order of the components results in a drastic increase in the concentrations when DNA is compacted. According to the suggested mechanism, after the formation of Ag-ME complex in the absence of DNA, no free Ag^+ ions remain that can bridge Ag-ME complex to DNA. Therefore, in the inverse mixing order, when ready, $(-Ag\text{-}S(R)-)_n$ is used to compact DNA; DNA compaction occurs at more than 100 times higher concentrations of $AgNO_3$. In other words, the formation of a large

dx.doi.org/10.1021/bm300277f | Biomacromolecules XXXX, XXX, XXX−XXX

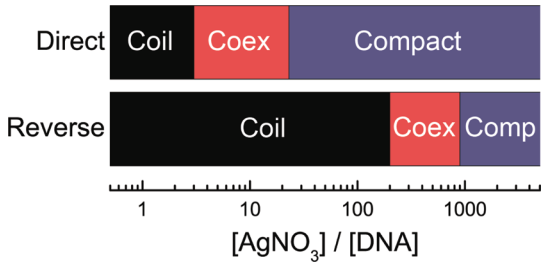

Figure 7. Dependence of the DNA conformational state on concentration of $AgNO_3$ in solution in the presence of equivalent amount of ME upon direct (1, DNA; 2, $AgNO_3$; and 3, ME) and reverse (1, ME; 2, $AgNO_3$; 3, DNA) orders of components mixing. Abbreviations Coil, Coex, and Comp refer to DNA in coil, coil–globule coexistence, and compact state, respectively.

complex containing limited number of positively charged sites is not efficient to interact electrostatically with DNA polyanion. Such a drastic dependence on the mixing order of $AgNO_3$ and ME justifies the proposed mechanism in Figure 6, indicating that initial intercalation of Ag^+ into DNA is essential for the efficient construction of $(-Ag\text{-}S(R)-)_n$ complex on DNA and induction of DNA compaction.

We also investigated the possibility of recovering DNA from Ag-ME complexes. We supposed that such unfolding could be realized by the addition of a stronger silver complexing agent, which does not polymerize into oligomeric sequences such as $(-Ag\text{-}S(R)-)_n$. Because ME forms strong complexes with silver, only a limited number of ligands such as I^- or S^{2-} can form complexes with a higher stability. In our experiments, we used Na_2S because it is known that binding of S^{2-} with Ag^+ is exceptionally strong (pK_{sp} = 49.1). Na_2S was added at varied concentrations into solution of DNA (1×10^{-8} M) compacted by $AgNO_3$ (1×10^{-6} M) and ME (1×10^{-5} M). Figure 8 shows the distributions of T4 DNA molecules' long-axis length before and after the addition of Na_2S (1×10^{-3} M) along with representative fluorescence microscopy images. Remarkably,

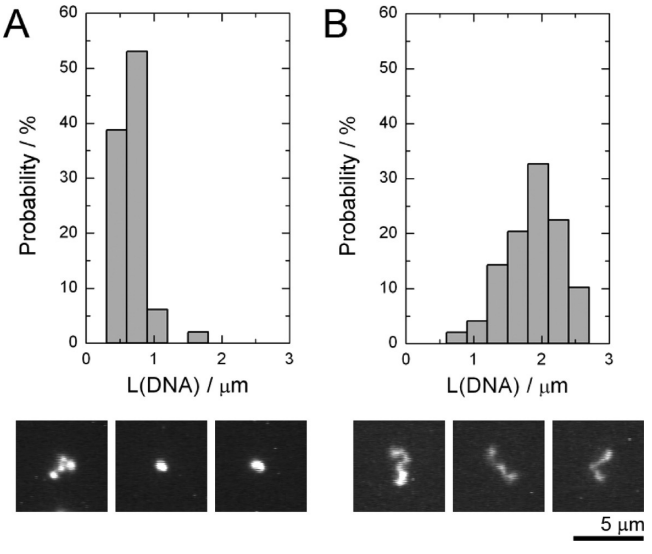

Figure 8. Histograms of T4 DNA size distribution (top) and typical fluorescence images (bottom) after the addition to the T4 DNA solution (1×10^{-8} M), $AgNO_3$ (1×10^{-6} M), and mercaptoethanol (1×10^{-6} M) before (A) and after (B) the addition of Na_2S (1×10^{-3} M).

after the addition of Na_2S to DNA-Ag-ME complex solution and incubation for 10 min prior to observation, all DNA molecules were found in the unfolded coil state (Figure 8B). Therefore, the formation of tricomponent DNA-Ag-ME complexes is reversible, and competitive formation of Ag^+ complexes with a stronger ligand than ME, which does not form polymeric chains, provokes a decomposition of the complex and a release of DNA from complexes.

Nanostructures Formed As a Result of Silver Complex Deposition on DNA Scaffold. Finally, the morphology of the $AgNO_3$ and ME complexes on DNA scaffold was studied by TEM. Representative TEM images of complexes formed in solutions of $AgNO_3$ and ME, in the absence and in the presence of T4 DNA, are shown in Figure 9. In solution without DNA, we observed 1D fiber-like structures of ~10 nm thickness (Figure 9A,A′). These fibers represent nanostructures of $(-Ag\text{-}S(R)-)_n$ polymers similar to 1D fibers previously reported for solutions containing silver and aromatic thiols.[19] Significant changes in fibers' morphology were observed when complex formation was carried out in the presence of T4 DNA (Figure 9B,B′). The thickness of fibers was increased up to about 20–30 nm, whereas the length of observed structures was limited by several hundred nanometers. Because the number of observed nanostructures shown in Figure 9B,B′ was significantly fewer than those in Figure 9A,A′ at the same concentrations of $AgNO_3$ and ME, we concluded that they are templated by DNA, which is compacted based on FM observations. An additional argument to support this conclusion is the 100–200 nm dimension of such condensates, which is a typical size for compact nanostructures formed by semiflexible DNA molecule. The composition of such aggregates is mostly $(-Ag\text{-}S(R)-)_n$ complex due to the excess of $AgNO_3$ and ME used for DNA compaction that grow on DNA template toward formation of thicker fibers. Indirect evidence supporting such mechanism can be found in Figure 4 at high concentrations of $AgNO_3$ and ME, where DNA seems to be included into the aggregates formed by a large quantity of polymerized $(-Ag\text{-}S(R)-)_n$.

The structures in Figure 9B,B′ correspond to the compact DNA structures in Figure 4B at concentration 1×10^{-6} M (100-fold excess of $AgNO_3$ and ME to DNA phosphates) because due to blurring effect in fluorescence microscopy, objects with linear dimension 200–300 nm appear as about 1 μm globules in FM with no regard to the complexity of their shape.

It is important to mention that fibers in Figure 9 are decorated with a small amount of nanoparticles with sizes below 10 nm, which, however, are not the product of DNA mineralization with Ag and ME but caused by silver complex reduction by an electron beam during TEM microscopy observations, which was confirmed by observation of their growth into larger particles at longer times of observation. Results of FM observation showing a decrease in DNA molecular volume with an increase in the concentration of $AgNO_3$ and ME together with the morphology of nanostructures observed by TEM suggest that nanostructures in Figure 9B,B′ are formed as a result of $(-Ag\text{-}S(R)-)_n$ complex formation on DNA scaffold that leads to DNA compaction.

CONCLUSIONS

The formation of silver complex with thiol induces highly efficient compaction of DNA chain into nanocomposite hybrid condensate. Compaction of DNA using the method presented

dx.doi.org/10.1021/bm300277f | Biomacromolecules XXXX, XXX, XXX–XXX

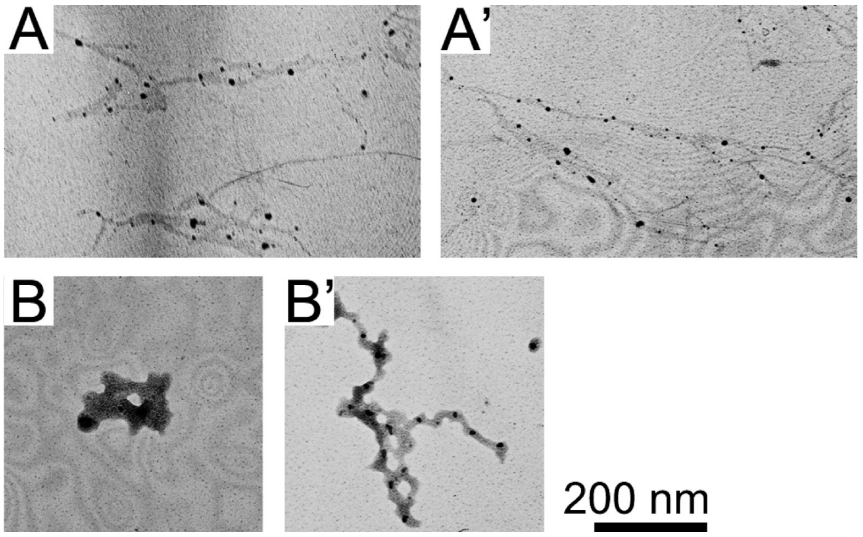

Figure 9. Transmission electron microscopy images of structures observed in samples prepared either by mixing of $AgNO_3$ (1×10^{-4} M) and ME (1×10^{-4} M) (A, A′) or by the addition of the same amounts of $AgNO_3$ and ME to T4 DNA (1×10^{-6} M) solution (B, B′). The dots on the complexes are formed due to silver reduction into Ag nanoparticles, as supported by time-resolved TEM observations.

here is reversible, and DNA can be released from the complex upon addition of ligands with a higher binding constant. Using the described method and by choosing appropriate ratio between DNA, Ag, and ME, one can construct at will tricomponent complexes, which chemical structure and properties can be controlled by tailoring a suitable thiol-containing functional group.

AUTHOR INFORMATION

Corresponding Author

*E-mail: zinchenko@urban.env.nagoya-u.ac.jp; sergeyev@genebee.msu.ru.

Notes

The authors declare no competing financial interest.

ACKNOWLEDGMENTS

We gratefully acknowledge the High Voltage Electron Microscope Laboratory at EcoTopia Science Institute, Nagoya University, and Dr. S. Arai for assistance with the TEM observations. This work was supported in part by KAKENHI 24710106 (Grant-in-Aid for Young Scientists (B) type).

REFERENCES

(1) Jones, M. R.; Osberg, K. D.; Macfarlane, R. J.; Langille, M. R.; Mirkin, C. A. Templated techniques for the synthesis and assembly of plasmonic nanostructures. *Chem. Rev.* **2011**, *111* (6), 3736−3827.

(2) Kwon, Y. W.; Lee, C. H.; Choi, D. H.; Jin, J. I. Materials science of DNA. *J. Mater. Chem.* **2009**, *19* (10), 1353−1380.

(3) Becerril, H. A.; Woolley, A. T. DNA-templated nanofabrication. *Chem. Soc. Rev.* **2009**, *38* (2), 329−337.

(4) Lu, J. J.; Yang, L. B.; Xie, A. J.; Shen, Y. H. DNA-templated photo-induced silver nanowires: fabrication and use in detection of relative humidity. *Biophys. Chem.* **2009**, *145* (2−3), 91−97.

(5) Atanasova, P.; Weitz, R. T.; Gerstel, P.; Srot, V.; Kopold, P.; van Aken, P. A.; Burghard, M.; Bill, J. DNA-templated synthesis of ZnO thin layers and nanowires. *Nanotechnology* **2009**, *20* (36), 365302.

(6) Nguyen, K.; Monteverde, M.; Filoramo, A.; Goux-Capes, L.; Lyonnais, S.; Jegou, P.; Viel, P.; Goffman, M.; Bourgoin, J. P. Synthesis of thin and highly conductive DNA-based palladium nanowires. *Adv. Mater.* **2008**, *20* (6), 1099−1104.

(7) Kundu, S.; Liang, H. Photochemical synthesis of electrically conductive CdS nanowires on DNA scaffolds. *Adv. Mater.* **2008**, *20* (4), 826−831.

(8) Fischler, M.; Simon, U.; Nir, H.; Eichen, Y.; Burley, G. A.; Gierlich, J.; Gramlich, P. M. E.; Carell, T. Formation of bimetallic Ag-Au nanowires by metallization of artificial DNA duplexes. *Small* **2007**, *3* (6), 1049−1055.

(9) Kinsella, J. M.; Ivanisevic, A. DNA-templated magnetic nanowires with different compositions: fabrication and analysis. *Langmuir* **2007**, *23* (7), 3886−3890.

(10) Gu, Q.; Cheng, C. D.; Haynie, D. T. Cobalt metallization of DNA: toward magnetic nanowires. *Nanotechnology* **2005**, *16* (8), 1358−1363.

(11) Lapierre-Devlin, M. A.; Asher, C. L.; Taft, B. J.; Gasparac, R.; Roberts, M. A.; Kelley, S. O. Amplified electrocatalysis at DNA-modified nanowires. *Nano Lett.* **2005**, *5* (6), 1051−1055.

(12) Monson, C. F.; Woolley, A. T. DNA-templated construction of copper nanowires. *Nano Lett.* **2003**, *3* (3), 359−363.

(13) Richter, J.; Mertig, M.; Pompe, W.; Monch, I.; Schackert, H. K. Construction of highly conductive nanowires on a DNA template. *Appl. Phys. Lett.* **2001**, *78* (4), 536−538.

(14) Jensen, R. H.; Davidson, N. Spectrophotometric potentiometric and density gradient ultracentrifugation studies of binding of silver ion by DNA. *Biopolymers* **1966**, *4* (1), 1732.

(15) Sissoeff, I.; Grisvard, J.; Guille, E. Studies on metal ions-DNA interactions: specific behaviour of reiterative DNA sequences. *Prog. Biophys. Mol. Biol.* **1976**, *31* (2), 165−199.

(16) Arakawa, H.; Neault, J. F.; Tajmir-Riahi, H. A. Silver(I) complexes with DNA and RNA studied by Fourier transform infrared spectroscopy and capillary electrophoresis. *Biophys. J.* **2001**, *81* (3), 1580−1587.

(17) Dirico, D. E.; Keller, P. B.; Hartman, K. A. The infrared-spectrum and structure of the type-I complex of silver and DNA. *Nucleic Acids Res.* **1985**, *13* (1), 251−260.

(18) Baena, M. J.; Espinet, P.; Lequerica, M. C.; Levelut, A. M. Mesogenic behavior of silver thiolates with layered structure in the solid-state - covalent soaps. *J. Am. Chem. Soc.* **1992**, *114* (11), 4182−4185.

(19) Dance, I. G.; Fisher, K. J.; Banda, R. M. H.; Scudder, M. L. Layered structure of crystalline compounds AgSR. *Inorg. Chem.* **1991**, *30* (2), 183−187.

(20) Andersson, L. Study of Some Silver-Thiol Complexes and Polymers - Stoichiometry and Optical Effects. *J. Polym. Sci., Part A* **1972**, *10* (7), 1963−1973.

(21) Hernandez, E. A.; Posada, B.; Irizarry, R.; Castro, M. E. Role of hydrogen bonding interactions in directing one-dimensional thiol-assisted growth of silver-based nanofibers. *J. Phys. Chem. B* **2005**, *109* (15), 7251−7257.
(22) Sailaja, S.; Rajasekharan, M. V. Synthesis and structure of coordination polymers of Ag(I) with isomeric (aminomethyl)-pyridines. Formation of a novel circular helicate and 2-D networks via Ag...Ag contacts and coordination shell expansion under anion control. *Inorg. Chem.* **2003**, *42* (18), 5675−5684.
(23) Tan, Y.; Jiang, L.; Li, Y.; Zhu, D. One Dimensional Aggregates of Silver Nanoparticles Induced by the Stabilizer 2-Mercaptobenzimidazole. *J. Phys. Chem. B* **2002**, *106* (12), 3131−3138.
(24) Sailaja, S.; Swarnabala, G.; Rajasekharan, M. V. Complexes of Ag-I with cationic ligands: bis[(pyridylmethyl)ammonio]silver(I) salts. *Acta Crystallogr., Sect. C* **2001**, *57*, 1162−1165.
(25) Sailaja, S.; Rajasekharan, M. V. One-dimensional coordination polymers of silver(I) with aminomethylpyridines. Example of a triple helical infinite chain. *Inorg. Chem.* **2000**, *39* (20), 4586−4590.
(26) Hong, M.; Su, W.; Cao, R.; Zhang, W.; Lu, J. Controlled assembly based on multibridging thiolate ligands: new polymeric silver(I) complexes with one-dimensional chain and three-dimensional network structures. *Inorg. Chem.* **1999**, *38* (3), 600−602.
(27) Fijolek, H. G.; GonzalezDuarte, P.; Park, S. H.; Suib, S. L.; Natan, M. J. Structure-spectroscopy correlations in silver thiolates: application to the structure of silver 1,5-pentanedithiolate. *Inorg. Chem.* **1997**, *36* (23), 5299−5305.
(28) Zinchenko, A. A.; Baigl, D. M.; Chen, N.; Pyshkina, O.; Endo, K.; Sergeyev, V. G.; Yoshikawa, K. Conformational behavior of giant DNA through binding with Ag+ and metallization. *Biomacromolecules* **2008**, *9* (7), 1981−1987.
(29) Cecil, R. The quantitative reactions of thiols and disulphides with silver nitrate. *Biochem. J.* **1950**, *47* (5), 572−584.
(30) Tunaboylu, K.; Schwarzenbach, G. Silver Mercaptides and Silver Mercapto Complexes. *Helv. Chim. Acta* **1971**, *54* (7), 2166−2185.
(31) James, T. H.; Mees, C. E. K. *The Theory of the Photographic Process*, 4th ed.; Macmillan: New York, 1977; p xvii, 714 p.